KKU Engineering Journal
http://www.en.kku.ac.th/enjournal/th/

Finite element simulation of a laser scribing process for a head suspension in hard disk drives

Teerawat Kumnorkaew and Vitoon Uthaisangsuk*

Department of Mechanical Engineering, King Mongkut's University of Technology Thonburi Bangkok, Thailand 10140

Received February 2012
Accepted June 2012

Abstract

Quality control in production process of head suspension plays an important role in Hard Disk Drive (HDD) manufacturing. In order to ensure an accurate read/write operation of hard disk, a major assembly step of flying height, a distance between disk surface and head, must be examined. Recently, laser scribing technique has been applied to alter flying height to desired values of Pitch Static Attitude (PSA) and Roll Static Attitude (RSA). These two parameters are used as industrial standard for production of hard disk drive. This study concerns a prediction of deformation behaviour of head suspension undergoing laser scribing process by means of Finite Element Analysis (FEA). Material properties of austenitic steel 304 customarily employed for the head suspension were investigated depending on temperature. Finite element simulations combined with an isotropic hardening as well as a non-linear kinematic hardening model were carried out in order to study material responses after the cyclic laser scribing. The results from simulations using those material models were compared with experimental results, in which the kinematic hardening model provided more accurate predictions.

Keywords: Laser scribing, Non-linear kinematic hardening, Head suspension,Flying height, Finite element analysis, Austenitic steel 304

1. Introduction

Laser scribing technique has been implemented to production of Hard disk Drive (HDD) in order to adjust configuration of slider such as pitch and roll of head suspension to desired positions. The process utilizes intermittent laser beam focused on the surface of head suspension arm to generate a rapid heating up and cooling down cycle. By this manner, residual stress and strain occurs for material in area subjected to this ther mal cycle. Due to the applied pulsating laser thermal stresses develop periodically on material surface that finally leads to a bending and twisting response of the head suspension. Drawing of a typical head suspension is illustrated in Fig. 1 with the slider placed at position zero (0). The alignment in space of the slider relative to suspension and disk can be determined by the values called Pitch Static Attitude (PSA) and Roll Static Attitude (RSA). In general, the PSA and RSA are

*Corresponding author. Tel.: +66-2470-9274 ; Fax: +66-2470-9111
Email address: vitoon.uth@kmutt.ac.th (V.Uthaisangsuk).

in conjunction with the pitch and roll angle, which are the angle rotating along line A-A and B-B, respectivly. Both parameters are used for describing the head suspension attitude after laser scribing process.

Laser scribing process has been included to different engineering operations like metal forming by laser, modifying metal surface, adjusting deformed sample, and forming of small sample. Many researchers have attempted to obtain an agreement between experimental and simulation results for the laser scribing procedure. Hsiao developed a Finite Element Analysis (FEA) based method for computing deformation of metal caused by laser heating [1] . The finite element model was used to determine an optimum heat for a specific deformation of low carbon steel (HY80) and hard steel (HSLA80). In 2000, Kelkar reported that material behaviour during pulsating laser was similar to the one during rapid quenching [2]. In 2007, Dutta Majumdar found that bending angle of sample after laser forming was the result of scanning rate, number of lines, and thickness of sample in addition to the heat flux [3] . Here, effects of thermal stress and laser irradiation on microstructure and phase transformation of a stainless steel were also studied. In 2009, Patangtalo studied laser scribing for adjusting a deformed head suspension of HDD [4]. In this study, effects of position, speed, and line of scribing on the deformation were investigated. However, experimental results did not agree well with finite element results. In 2010, Yang studied behaviour of stainless steel 304 in terms of microstructure, micro hardness and spring back properties after laser scribing [5]. Tsuchida and his co-workers [6] described effect of temperature on the static tensile properties of the metastable austenitic steel 304 in order to clarify the conditions of stress-induced martensitic transformation behaviour for maximum uniform elongation.

In this work, finite element analysis was applied aiming to predict material behaviour of alaser-scribed sample and to eliminate production defects. For this purpose, an effective finite element model was developed under consideration of major material factors affecting calculation of residual stress such as flow curves and thermal expansion of material. Generally, head suspension in hard disk drive is made of stainless steel 304 (AISI304). This metastable austenitic steel grade can exhibit a phase transformation from austenite to martensite when a proper condition of load and temperature is provided. The transformation initiates a volume expansion about 3% resulting in additional residual stress in the sample. Furthermore, effect of cyclic hardening phenomena occurred due to thermal stress cycle induced by pulsating laser on deformation behaviour of a head suspension was considered. The cyclic behaviour was described by introducing a non-linear kinematic hardening model. Elastic and plastic mechanical properties of metastable austenitic steel 304 were taken from a material database for the simulations [7] . In this work, the finite element calculations were assumed to be a 3D-coupling thermo-elasto-plastic problem. Numerical results regarding the static attitude of sample obtained from non-linear kinematic hardening analysis and isotropic hardening analysis were then compared with experimental results for different laser speeds and number of scribing line. By incorporating these all deformation mechanisms of the head suspension during laser scribing a more accurate finite element model can be provided.

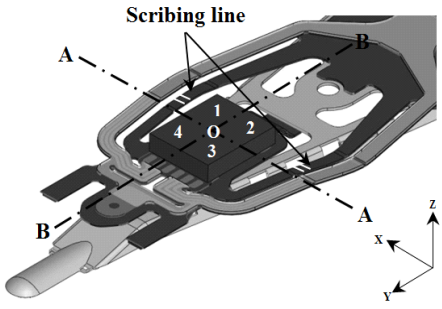

Figure 1 Drawing of head suspension

2. Experimental procedure

In this study, there are two major investigations that are described as followed.

2.1 Material

Head suspension is principally manufactured using a stainless steel grade 304 (AISI304). Thus, it was necessary to study material properties and behaviours of the metastable austenitic steel 304 under defined laser scribing conditions. In this work, a commercial steel sheet AISI304 with a thickness of 0.2 mm was taken. The chemical composition of the examined austenitic steel is given in Table 1. This composition was proven to be in the range of steel used for the head suspension, especially Cr and Ni content. Figure 2 shows typical stress-strain curves of austenitic steel 304 obtained by Tsuchida for different temperatures between -150 °C and 100 °C [6]. The stress-strain curves represent an extraordinary strengthening mechanism due to the trans¬formation-induced plasticity (TRIP effect), by which the metastable austenitic phase transforms to martensitic phase when a critical strain is reached. Laser scribing with similar condition for head suspension was performed for the steel plate, in order to determine this TRIP effect caused by temperature change and deformation of the sample.

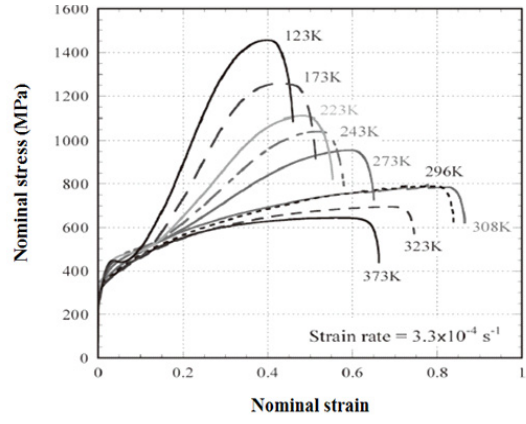

Figure 2 Nominal stress-strain curves obtained by static tensile test at various temperatures for AISI304 steel [6]

Table 1 Chemical compositions of the Investigated austenitic- steel AISI304 (mass%)

C	Si	Mn	P	s	Ni	Cr	Cu
0.06	0.56	0.95	0.03	0.01	7.55	17.95	0.35

2.2 Laser scribing process

A laser type of Nd:YAG (Neodymium-doped yttrium aluminium garnet; Nd:$Y_3Al_5O_{12}$) was applied as the energy source. The pulsating laser has a power of 0.45 W with a beam diameter of 13 μm. The frequency and dwell time of each pulse acting to sample surface is 1 kHz and 50 ns, respectively. Locations of scribing line on both arms of the suspension are indicated in Figure 1. Note that the number of scribing line conducted in the experiment could be either one or two on each side in order to gain a wider range of pitch angle adjustment. The direction of scribing lines was perpendicular to the edge of outer arm and was directed inward across each arm. The cross section of the arm underneath the laser irradiated line was 111×20 μm^2 in width and thickness directions, respectively. The single line on each side was scribed at the speed of 50 mm/s and

100 mm/s, while the double lines were scanned at the same speeds with the distance of 200 μm between both lines. Only pitch angle could be adjusted if both arms were scanned exactly by the same manner, whereas both pitch and roll angles were adjusted if different scan parameters, for example, number of scribing line or speed, were applied to both suspension arms. The PSA and RSA of the suspension could be evaluated by measuring the coordinate positions of the attached slider according to points 1, 2, 3, and 4 in Figure 1 for the state before and after laser scribing.

3. Numerical FE simulation

Concerning the laser scribing process, FE simulations for thermal and mechanical problem were successively carried out. First, temperature field was computed and taken as a boundary condition for following stress analysis. In the simulations for thermal analysis, laser heat source was considered as laser intensity distribution leading to intermittent temperature in each step. The laser intensity according to the Gaussian mode as shown in Eq. (1) was calculated.

$$q(r) = \frac{2\eta P}{\pi R^2}\exp(-\frac{2r^2}{R^2}) \qquad (1)$$

Where q is heat flux density, η is heat absorbing effectiveness of material, *P* is laser power, R is laser beam radius, and r is distance from centre of the laser beam. In Eq. (1) it can be seen that the power of laser regarded in the Gaussian mode is not what indicated by CW laser specification of the Q-switch technique. Therefore, the power in Eq. (1) needed to be adjusted by scaling up to accommodate the Q-switch pulsed frequency of 1 kHz and dwell time of pulse of 50 ns. Initial temperature of the head suspension was given to be room temperature (25°C). Boundary surfaces of the suspension were subjected to heat convection and radiation with a convective heat transfer coef

ficient h_f of 25 W/m2 and a radiative heat transfer coefficient er of 0.4 W/m2K4

In simulations for stress analysis, temperature distribution on the head suspension obtained from the thermal analysis was taken into account. Here, energy of the laser beam was transferred to suspension arm, in which thermal expansion and contraction of material caused thermally induced stress in the heat affected zone. To compute this thermal stress and strain, material properties such as young's modulus, material density, plastic stress-strain curves as a function of temperature, and gravity load were given. The plastic stress-strain responses taken from database [7] as represented in Figure 3 were used.

In case of material subjected to cyclic loading, kinematic hardening model should be considered for describing deformation behaviour of the material. A nonlinear isotropic/kinematic model coupling with the Von Mises yield criterion was used for the stress analysis simulation [8] . Also, the pressure-independent yield surface is defined as:

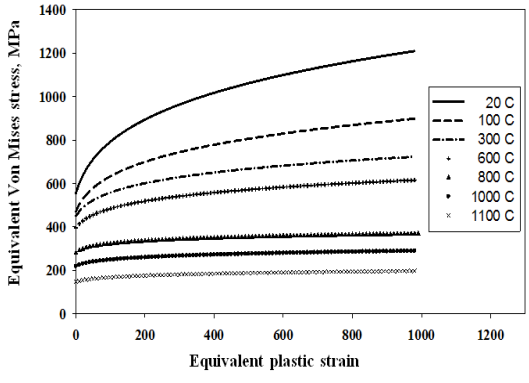

Figure 3 True stress-strain relation of AISI304 steel for different temperatures from a material database[7]

$$F = f(\sigma - \alpha) - \sigma^0 = 0 \quad (2)$$

Where σ^0 is yield stress and $f(\sigma - \alpha)$ is equivalent Von Mises stress with respect to back stress . For a stress increase in plastic range, position of the centre of the yield surface can be described as followed:

$$\dot{\varepsilon}^{pl} = \dot{\bar{\varepsilon}}^{pl}\left(\frac{\partial F}{\partial \sigma}\right) \quad (3)$$

Where $\dot{\varepsilon}^{pl}$ is the rate of plastic flow and $\dot{\bar{\varepsilon}}^{pl}$ is the equivalent plastic strain rate according to the Von Mises yield criterion. The applied hardening model consists of two components: a nonlinear kinematic hardening component, which describes the translation of yield surface in stress space through the back stress α and an isotropic hardening component, which represents the change of equivalent stress defining size of the yield surface σ^0 as a function of plastic deformation. Both hardening components are illustrated in Figure 4. The nonlinear kinematic component is defined as an additional combination of a purely kinematic term or linear Ziegler hardening law as given in Eq. (4) and a relaxation term, which introduces the nonlinearity [8] .

$$\dot{\alpha} = C\frac{1}{\sigma^0}(\sigma - \alpha)\dot{\bar{\varepsilon}}^{pl} \quad (4)$$

Where C is the kinematic hardening modulus. In addition to this equation backstress is superposed that can considerably improve results for the laser scribing process. The combined term in the nonlinear kinematic model is expressed as:

$$\dot{\alpha}_k = C_k\frac{1}{\sigma^0}(\sigma - \alpha)\dot{\bar{\varepsilon}}^{pl} - \gamma_k\alpha_k\dot{\bar{\varepsilon}}^{pl} \quad (5)$$

Where C_k and γ_k are material parameters that must be calibrated from cyclic testing data. C_k is the initial kinematic hardening modulus and γ_k determine the rate at which the kinematic hardening modulus decreases with increasing plastic deformation [8] .

The FE model with its corresponding meshing is shown in Figure 5. It should be noted that the model does not include the whole head suspension body in order to reduce computational time. Only region in the vicinity of the scribing zone was significantly affected by temperature change and deformation. Therefore, in the FE model much finer mesh was defined for this area on both suspension arms. The smallest element size was 5 x 6 x 2 μm. Element type used in the model of was eight-node brick element for both thermal and stress analysis.

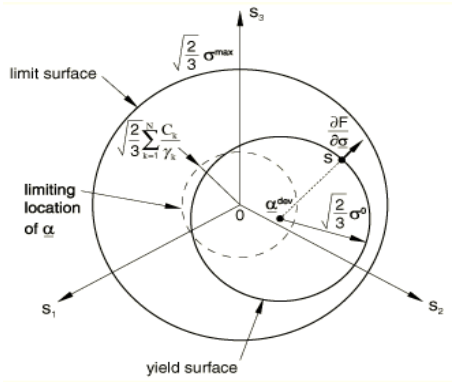

Figure 4 Three-dimensional representation of the hardening in a nonlinear isotropic/kinematic model[8]

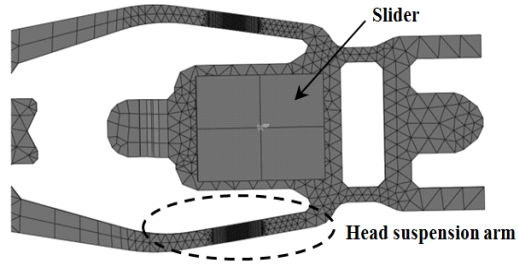

Figure 5 FE model for head suspension including slider

For the verification, the PSA of the head suspension after laser scribing was calculated with respect to the positions illustrated in Figure 1. The equations can be expressed as:

$$S_{xx} = [\frac{(x_1^2 + x_2^2 + x_3^2 + x_4^2) - 4x_b^2}{3}] \quad (6)$$

$$S_{yy} = [\frac{(y_1^2 + y_2^2 + y_3^2 + y_4^2) - 4y_b^2}{3}] \quad (7)$$

$$x_b = \frac{(x_1 + x_2 + x_3 + x_4)}{4} \quad (8)$$

$$y_b = \frac{(y_1 + y_2 + y_3 + y_4)}{4} \quad (9)$$

$$z_b = \frac{(z_1 + z_2 + z_3 + z_4)}{4} \quad (10)$$

$$S_{xy} = [\frac{(x_1y_1 + x_2y_2 + x_3y_3 + x_4y_4) - 4x_by_b}{3}] \quad (11)$$

$$S_{yz} = [\frac{(y_1z_1 + y_2z_2 + y_3z_3 + y_4z_4) - 4y_bz_b}{3}] \quad (12)$$

$$S_{zx} = [\frac{(z_1x_1 + z_2x_2 + z_3x_3 + z_4x_4) - 4z_bx_b}{3}] \quad (13)$$

$$\beta = \frac{[(S_{yz} \times S_{xx}) - (S_{xy} \times S_{zx})]}{[(S_{xx} \times S_{yy}) - S_{xy}^2]} \quad (14)$$

$$PSA = \tan^{-1} \beta \quad (15)$$

4. Results and discussion

An attempt was done to qualitatively identify stress-induced martensitic transforma-tion in the sheet sample of steel AISI304 after corresponding laser scribing test. In this work, X-Ray Diffraction (XRD), which is a non-destructive technique that can reveal detailed information about the crystallographic structure of a material, was applied. The XRD analysis was conducted for the plate sample and a first result is presented in Fig. 6. The diffraction range 2θ was set to be from 20° to 80°. The main peaks observed in the XRD spectra are γ (001), γ (111), γ (200), γ (220), and α' (001). There is a small hint of phase transformation. Nevertheless, it must be confirmed by further metallographic investigation. With respect to numerical results, deformation mechanism of the head suspension could be explained.

When a laser beam with high power moved through the top surface of material in the form of pulsating heat flux, the material would absorb a part of energy on this surface. Then, heat energy was transferred to the material. This energy was distributed non-uniformly along the suspension arms due to the Gaussian mode of the pulsating heat flux.

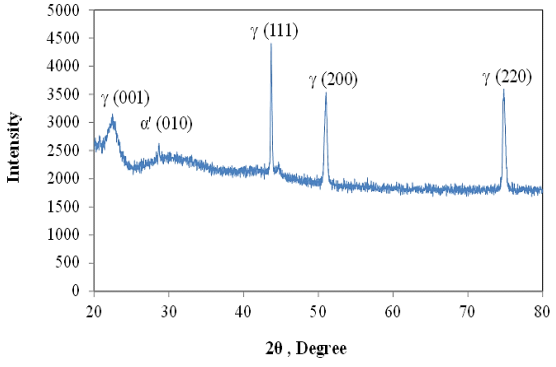

Figure 6 Resulted X-ray diffraction pattern of a sheet specimen of steel AISI304 after laser scribing test

On the top surface of head suspension arm heat intensity was higher than the bottom surface. This effect consequentially led to a more expansion of material at the top surface than material at the respective underneath area. As a result, the head suspension arm was formed in a counter V shape. This resulted deformation was due to elastic tensile strain on the top surface and subsequent compressive stress affected by the constraint of adjacent cooler material zone on

the bottom surface.This compressive stress was a consequence of the plastic deformation. The process of laser scribing would be more effective when finally the thermal expansion of material gave rise to a plastic strain rather than elastic strain. In contrast, when the laser beam passed any area, material in this area becamecoolandheattransferinthematerialbecameless. Thus, the head suspension arm shrunk and compressive stress and tensile strain was generated on the top and bottom surface, respectively. In this case, the deformed head suspension arm was a V shape. Obviously, deformation mechanism of the head suspension duringlaserscribingprocessexhibitedacyclicbehaviour. The kinematic hardening model was introduced in finite element calculations for describing this material behaviour.

Finite element simulations for various cases as mentioned in the previous section were performed. In Figure 7 calculated temperature development for a midpoint on the top and bottom surface of the left suspension arm was plotted against scribing time up to 5 ms, when the laser beam just left the left arm. At the scribing speed of 50 mm/s there were totally five laser pulses along a suspension arm per one scan. After 1 ms the first laser pulse completely reached the left arm. Subsequently, when the next laser pulses irradiated on the surface, the temperature on the suspension arm was superposed. As a result, overall temperature on the suspension arm became higher. The maximum temperature peak on the midpoint of the left arm was about 2600°C, which was higher than the melting point of material. However, this temperature peak took place for a short time, because the head suspension is so thin and the material can be afterwards cooled down very quickly.

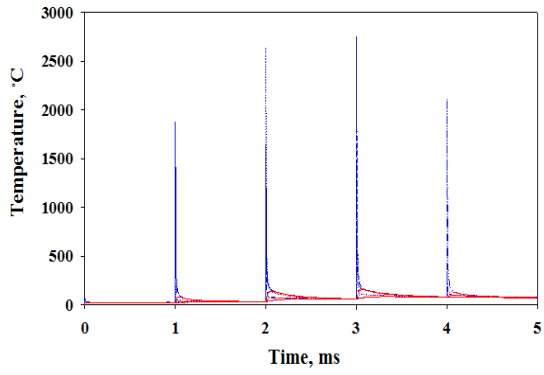

Figure 7 Calculated temperature development for a midpoint on the top and bottom surface of the left suspension arm up to a scribing time of 5 ms

Calculated results of single scribing line with ascribingspeedof50mm/swereshownforbothhardening models in Figure 8. In this figure equivalent compressive stresses on the top surface of the head suspension arm were plotted against distance in x-direction along both suspension arms at the end of the scribing process (after 60 s). It is noticed that simulation using isotropichardeningmodelcomputedconsiderablyhigher residual stresses than simulation using kinematic hardening model. Stress distribution obtained from isotropichardeningmodelwassimilarforbothsuspension arms, but kinematic hardening model computed lower stress magnitude for the left arm, since the laser pulse moved throughout from the left to the right arm. When applying kinematic hardening, residual stress initially occurred on the left arm apparently influenced stress developed later on the right suspension arm.left arm, since the laser pulse moved throughout from the left to the right arm. When applying kinematic hardening, residual stress initially occurred on the left arm apparently influenced stress developed later on the right suspension arm.

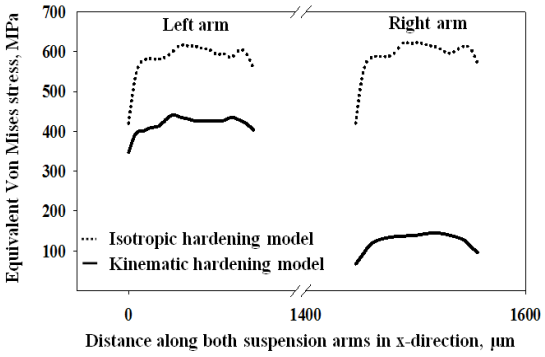

Figure 8 Calculated equivalent Von Mises stress for the top surface along both suspension arms in x-direction

In Figure 9 equivalent Von Mises stresses on the top and bottom surface of the head suspension along distance in x-direction of the left suspension arm at the end of the process were presented for both applied hardening models. Generally, the isotropic hardening model resulted in higher stress than the kinematic hardening model. On the top surface of the suspension arm compressive residual stress was generated, while tensile stress occurred on the bottom surface.

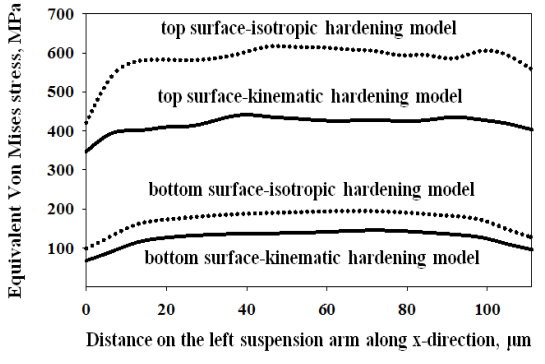

Figure 9 Calculated equivalent Von Mises stress for the top and bottom surface of the left suspension arm along x-direction

Figure10 shows computed equivalent strain distribution on the top surface of both suspension arms along x-direction. The strain distribution caused by pulsating laser in case of isotropic hardening analysis was higher than kinematic hardening analysis. Predicted strain distributions on top and bottom surface of left suspension arm are illustrated in Figure 11. It can be seen that on both top and bottom surfaces, the kinematic hardening model provided a lower strain magnitude and the top surface exhibited higher strain values than the bottom surface because of significant temperature difference.

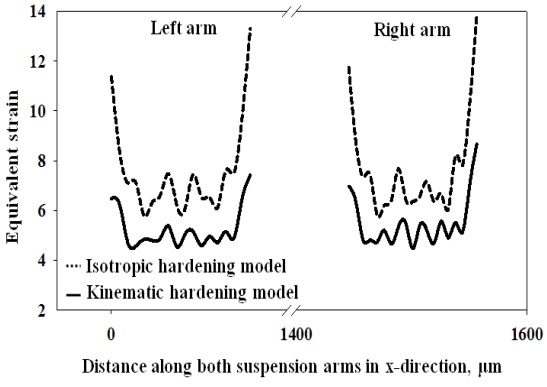

Figure 10 Computed strain distribution on the top surface along both suspension arms in x-direction

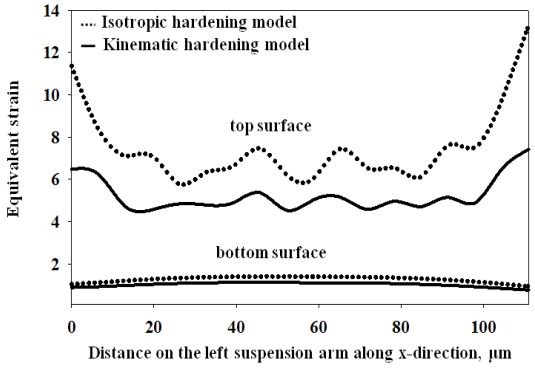

Figure 11 Computed strain distribution on the top and bottom surface of the left suspension arm along x-direction

Experimental results with regard to the PSA of the head suspension after laser scribing were summarized for different conditions in Figuer 12. The more number of scribing line used, the higher PSA value was obtained, since residual plastic strain was generated for a larger region. Furthermore, the magnitude of PSA could be increased by lowering scanning speed of the laser beam.

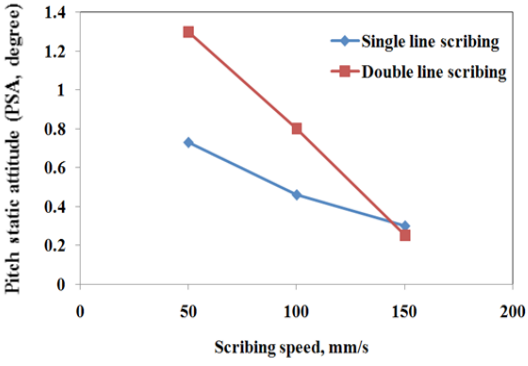

Figure 12 Effect of scribing speed and number of scribing line on the PSA of the suspension arm

Table 2 Error of PSA values predicted by isotropic and kinematic hardening model in comparison

Line number	Speed (mm/s)	Error (%)	
		Kinematic hardening	Isotropic hardening
1	50	7.89	22.63
1	100	11.78	28.82
1	150	14.26	45.43
2	50	9.03	14.03
2	100	8.26	12.65
2	150	2.52	12.44

Table 2 presents deviations in percentage between experimentally measured and numerical calculated pitch static attitude (PSA) of the head suspension after laser scribing process. In conclusion, the predicted results obtained from the kinematic hardening model were in a better agreement with the experimental results than the isotropic hardening model for all scribing conditions.

5. Conclusions

This study concerns a finite element modeling approach for describing deformation behavior of the head suspension under cyclic loading caused by pulsating laser. For this purpose, thermal and subsequent stress analysis of the laser scribing process was performed. Material properties of the austenitic steel AISI304 depending on temperature were considered in the finite element simulations. The metastable austenitic steel can exhibit an extraordinary strain hardening behavior when the TRIP effect occurs. Here, austenite-martensite transforma-tion takes place that leads to a volume expansion of 3%. An attempt was done to characterize the TRIP effect in steel 304 under pulsating laser condition. Isotropic hardening model and nonlinear kinematic hardening model were investigated with respect to the prediction of PSA of the head suspension. It was found that finite element simulations coupling with the kinematic hardening provided more accurate prediction results. Having a precise adjustment of the pitch and roll angle of the head suspension will significantly facilitate the production process of hard disk drive for both time and cost factors.

6. Acknowledgment

This work could not be performed without the research fund supported by the Industry/University Cooperative Research Centre in HDD Advanced Manufacturing and National Electronics and Computer Technology Centre, National Science and Technology Development Agency, as well as technical information supported by Western Digital (Thailand) Co, Ltd and Iron and steel Institute of Thailand. All supports are gratefully acknowledged by the authors.

7. References

[1] Y.C. Hsiao and W. Maher, “Finite elment modeling of laser forming,” in Proc. ICALEO, section A, 1980, p. 31–40.

[2] G. Kelkar, “PULSED LASER WELDING”, in SOJOM 2000, vol. 3, pp.256-262, Dec. 2000.

[3] J. Dutta Majumdar, A.K. Nath and I. Manna, “Studies on laser bending of stainless steel”,Mate rials Science and Engineering, vol. A385, pp.113–122, Nov. 2004.

[4] W. Patangtalo, S. Aimmanee, and S. Chuti ma.,2009, “Deformations of a suspension in a hard disk drive caused by laser scribing process”, M. Eng. Thesis under University Cooperative Re search Center in HDD Component (I/UCRC in HDD Component), KMUTT, Thailand, 2008.

[5] L.J. Yang, J. Tang, M.L. Wang, Y. Wang, and Y.B. Chen, “Surface characteristic of stainless steel sheet after pulsed laser forming”, Applied Surface Science , vol. 256, pp.7018–7026, Sep. 2010.

[6] N. Tsuchida, Y. Morimoto, T. Tonan, Y. Shibata, K. Fukaura, and R. Ueji, “Stress-Induced Marten sitic Transformation Behaviors at Various Temper atures and Their TRIP Effects in SUS304 Metasta ble Austenitic Stainless Steel”, ISIJ International, 2011;51(1):124–129.

[7] Material database of FE software DEFORM-3D.

[8] ABAQUS 6.10 Analysis User’s Manual, “Model for metals subjected to cyclic loading”, Section 19.2.2.